

*e.1*

Presented at the  
Berkeley APS meeting  
of the Division of  
Particles and Fields  
August 13-17, 1973

THRESHOLD EFFECTS AND OSCILLATIONS IN MODELS  
WITH  $t$ -CHANNEL FACTORIZATION

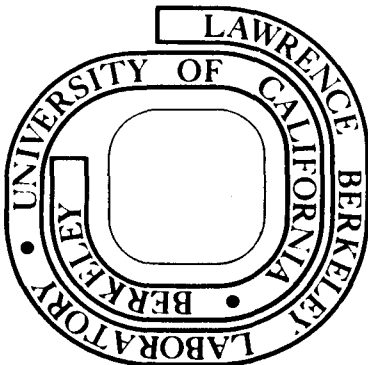
Joel Koplik

September 26, 1973

Prepared for the U. S. Atomic Energy Commission  
under Contract W-7405-ENG-48

**For Reference**

Not to be taken from this room



*e.1*  
LBL-2175

## **DISCLAIMER**

This document was prepared as an account of work sponsored by the United States Government. While this document is believed to contain correct information, neither the United States Government nor any agency thereof, nor the Regents of the University of California, nor any of their employees, makes any warranty, express or implied, or assumes any legal responsibility for the accuracy, completeness, or usefulness of any information, apparatus, product, or process disclosed, or represents that its use would not infringe privately owned rights. Reference herein to any specific commercial product, process, or service by its trade name, trademark, manufacturer, or otherwise, does not necessarily constitute or imply its endorsement, recommendation, or favoring by the United States Government or any agency thereof, or the Regents of the University of California. The views and opinions of authors expressed herein do not necessarily state or reflect those of the United States Government or any agency thereof or the Regents of the University of California.

THRESHOLD EFFECTS AND OSCILLATIONS IN MODELS  
WITH  $t$ -CHANNEL FACTORIZATION\*†

Joel Koplik

Lawrence Berkeley Laboratory, University of California  
Berkeley, California 94720

ABSTRACT

We review threshold effects and oscillating cross sections in the context of models (such as the multiperipheral) which employ factorization and indefinite repetition in the  $t$ -channel. The origin of logarithmic energy thresholds is illustrated by the ABFST model and applied to antibaryon production and rising cross sections at high energy. We then discuss large-mass diffraction dissociation and argue that this process is not responsible for the increase in the  $p$ - $p$  total cross section at ISR energies.

I. INTRODUCTION

Recent experimental results from ISR have shown an unexpected energy dependence in (at least) two quantities: the production of antibaryons and the  $p$ - $p$  total cross section. One interpretation of these phenomena, suggested by Sivers and von Hippel,<sup>1</sup> Suzuki,<sup>2</sup> and by Gaisser and Tan,<sup>3</sup> is to regard the former as a threshold effect and the latter as its consequence. We will review the origin of dynamical thresholds in multiperipheral models and their application to particle production and rising cross sections. A somewhat similar idea concerns the "threshold" for large-mass diffraction dissociation; we shall argue that such a mechanism does not involve a genuine threshold and cannot account for the increasing  $p$ - $p$  total cross section. The unpublished work discussed here has been carried out in collaboration with M. Bishari and G. F. Chew and will be fully reported elsewhere.

II. MULTIPERIPHERAL THRESHOLDS

The origin of the threshold effects which concern us is clearly exhibited by the pion-exchange multiperipheral model. The absorptive part of the elastic scattering amplitude is there given by the sum indicated in Fig. 1, where the horizontal links on the right are off-shell pions of squared-mass  $t_i$  and the circles represent  $\pi\pi$  absorptive parts of subenergy  $s_i$ . Algebraically this can be

\*Supported by the U.S. Atomic Energy Commission.

†Talk presented at the 1973 Berkeley meeting of the Division of Particles and Fields, APS.

written<sup>4</sup>

$$\begin{aligned}
 A(s,0) &\propto \sum_N \int ds_A ds_1 \cdots ds_B dt_0 \cdots dt_N \\
 &\times \frac{A_{\pi A}(s_A; t_0) A_{\pi\pi}(s_1; t_0, t_1) \cdots A_{\pi B}(s_B; t_N)}{(t_0 - m_\pi^2)^2 \cdots (t_N - m_\pi^2)^2} \\
 &\times \frac{1}{N!} (Y - q_A - q_1 - \cdots - q_B)^N \theta(Y - q_A - q_1 - \cdots - q_N - q_B)
 \end{aligned}
 \tag{1}$$

after some internal integrations. The  $q_i$  and  $Y$  are Lorentz boosts defined by

$$\begin{aligned}
 \cosh Y &= \frac{s - m_A^2 - m_B^2}{2m_A m_B} \\
 \sinh q_{A,B} &= \frac{s_{A,B} - m_{A,B}^2 - t_{0,N}}{2m_{A,B} \sqrt{-t_{0,N}}} \\
 \cosh q_i &= \frac{s_i - t_{i-1} - t_i}{2\sqrt{t_{i-1} t_i}}
 \end{aligned}
 \tag{2}$$

The step-function expresses energy conservation, and requires that the Lorentz boost  $Y$  from the rest frame of particle  $A$  to that of particle  $B$  be at least as large as the sum of the corresponding boosts  $q_i$  across each of the pion absorptive parts.

Since this is a multiperipheral model the  $t_i$  should be small, and we shall suppose that the combination of propagators and off-shell damping of the pion absorptive parts is such as to impose an effective cut-off

$$|t_i| \leq T \ll m^2$$

In this expression  $m$  is the lowest important mass in the pion absorptive part; in the  $\pi\pi$  case, for example, we have  $m \approx m_\rho$ .

This implies

$$\cosh q_i \gtrsim \frac{m^2}{2T},$$

so that energy conservation requires

$$Y \gtrsim q_A + q_B + N \log \frac{m^2}{T}, \quad (3)$$

and thus the increment in rapidity for adding another link is

$$\Delta \approx \log \frac{m^2}{T}.$$

For future use, note that this threshold effect is more pronounced for large  $m$ . A similar argument can be made for any multiperipheral model,<sup>5</sup> which is essentially why these models give a logarithmic energy dependence of the multiplicity.

### III. ANTIBARYON PRODUCTION

We will now apply these ideas to antibaryon production at high energy, showing how the threshold indicated by experiment can be understood in terms of our simple pion-exchange model. The experimental antibaryon cross section as a function of energy is shown in Fig. 2,<sup>6,7</sup> and may be roughly characterized as negligible below  $s \approx 150 \text{ GeV}^2$ , and substantial and increasing approximately linearly in  $\log s$  once the threshold is reached. A second important experimental fact<sup>6</sup> is that antibaryons are produced almost exclusively in the central region of rapidity, and not in association with the leading particles. Since antibaryons must be produced in  $\bar{B}\bar{B}$  pairs, whose mass is quite large in comparison with typical meson masses, the multiperipheral threshold mechanism just described immediately suggests itself. In the model above, antibaryon production is easily incorporated by assuming it occurs effectively through a  $\bar{B}\bar{B}$  resonance (or collection of resonances) near the kinematic threshold ( $2m_{\bar{B}}$ ) in the  $\pi\pi$  cross section, and that this resonance does not appear at the ends of the multiperipheral chain. The effective, dynamical threshold for  $\bar{B}$  production in p-p collisions is then the threshold for the process shown in Fig. 3, which from Eq. (3) is

$$Y_{th} = 2q_{\pi p} + q_{\bar{B}\bar{B}}$$

where

$$\sinh q_{\pi p} = \frac{\sqrt{T}}{2m_p},$$

$$\cosh q_{\bar{B}\bar{B}} = \frac{(2m_B)^2}{2T}.$$

Using  $T = 0.04 \text{ GeV}^2$  (obtained from experimental measurements of n-p backward elastic scattering, which is controlled by pion exchange) we find  $Y_{th} \approx 5.0$ . This result corresponds nicely to

$\log \frac{150 \text{ GeV}^2}{m_p^2}$ , so our simple model supports the proposal of Refs.

(2) and (3). The magnitude of the  $\bar{B}$  production cross section is determined in the pion-exchange model by the cross section for the process  $\pi\pi \rightarrow \bar{B}\bar{B}$ . We have verified<sup>8</sup> that the measured value of this latter cross section is indeed of the order of magnitude to account for the experimental results on  $\bar{B}$  production in p-p collisions.

To estimate the effect of  $\bar{B}$  production on the total cross section, it is convenient to use a further simplification of the multiperipheral model which approximates the sum over all partial cross sections which do not involve a  $\bar{B}\bar{B}$  pair by the leading Regge pole generated by the corresponding partial kernel. We assume this leading pole is located at  $J = \alpha_0$ , and it will be seen momentarily that consistency requires  $\alpha_0 < 1$ . Then the production of, e.g., two  $\bar{B}\bar{B}$  pairs, given by a sum of diagrams like those of Fig. 4a, is approximated by Fig. 4b. In addition we replace the integrated  $\pi\pi \rightarrow \bar{B}\bar{B}$  kernel by a coupling constant ( $g$ ) and reduce the problem to the form of Ref. (5), by assuming the minimum rapidity intervals on the ends of the chain to be the same as the internal intervals ( $\Delta$ ). Then the N- $\bar{B}\bar{B}$  pair absorptive part in A-B elastic scattering is

$$\begin{aligned} A^{(N)}(Y) &= \int_{\Delta}^Y dy_1 \cdots \int_{\Delta}^Y dy_{N+1} \delta \left( Y - \sum_{i=1}^{N+1} y_i \right) \\ &\quad \times \beta_A e^{\alpha_0 y_1} g e^{\alpha_0 y_2} g \cdots g e^{\alpha_0 y_{N+1}} \beta_B \cdots (4) \\ &= \beta_A \beta_B e^{\alpha_0 Y} \frac{1}{N!} \left[ g \left( Y - (N+1)\Delta \right) \right]^N \theta \left( Y - (N+1)\Delta \right), \end{aligned}$$

where the  $y_i$  are rapidity differences and  $\beta_{A,B}$  are Regge residues. The corresponding  $\sigma^{(N)}(Y)$  are shown in Fig. 5.

To examine the asymptotic behavior of  $\sigma_{tot}$ , it is convenient to go to the J-plane. We have

$$A^{(N)}(J) \equiv \int_0^\infty dY e^{-JY} A^{(N)}(Y)$$

$$= \beta_A \beta_B g^N \left( \frac{e^{-\Delta(J-\alpha_0)}}{J - \alpha_0} \right)^{N+1}, \quad (5)$$

and the complete absorptive part is

$$A(J) \equiv \sum_{N=0}^{\infty} A^{(N)}(J)$$

$$= \frac{\beta_A \beta_B e^{-\Delta(J-\alpha_0)}}{J - \alpha_0 - g e^{-\Delta(J-\alpha_0)}}. \quad (6)$$

The singularities of  $A(J)$ , which are the zeros of the denominator of (6), are a real pole above  $\alpha_0$  and an infinite sequence of complex poles to the left (see Fig. 6). The leading pole determines the asymptotic behavior of the total cross section (constant or decreasing power) and the complex poles reproduce the threshold behavior of Fig. 5, which appears as oscillations in  $\sigma_{tot}$ . The ratio of real to imaginary part of the amplitude also oscillates, roughly  $90^\circ$  out of phase with  $\sigma_{tot}$  (see Fig. 7). Note that the complex poles and resulting oscillations only arise if  $\Delta \neq 0$ ; a genuine threshold is required. As shown in Ref. (3), if the parameters in Eqs. (4) - (6) are chosen to reproduce the B cross section and an asymptotically constant  $\sigma_{tot}$ , there results an increase in  $\sigma_{tot}$  of 5-10% above the first  $\bar{B}$  threshold. One also finds a leading pair of complex poles at  $J \sim \frac{1}{2} \pm i$ , and this pair plus the leading real pole gives an excellent approximation for  $Y \gtrsim 2$ .

This result is in rough agreement with the rise in the p-p total cross section,<sup>9</sup> and if this mechanism is indeed the explanation the increase is seen as a transient effect and, barring new

important thresholds ( $d\bar{d}$  pairs?), the cross section should level off and gently oscillate to a nonincreasing asymptotic behavior.

For this to be a satisfactory explanation, one must ask why this particular threshold is so important. We suggest that there are two reasons:

1. The large mass of a  $B\bar{B}$  system and the absence of  $\bar{B}$ 's as leading particles delays their appearance to a rather high energy when the total cross section has otherwise settled down.

2. The large magnitude of the  $\pi\pi \rightarrow B\bar{B}$  cross section near the  $B\bar{B}$  threshold reflects an unusual concentration of resonances in this neighborhood.<sup>8</sup> These resonances are associated with the long-range pion exchange force that acts in the  $B\bar{B}$  channel but which does not act in two-meson channels (such as  $\pi\pi$ ,  $K\bar{K}$ , or  $\rho\rho$ ). These resonances arise from the (nonrelativistic potential) mechanism that produces the low kinetic energy states of classical nuclear physics. Such a mechanism is usually ignored in high energy physics, but it has been shown to be responsible for the large  $B\bar{B}$  cross sections at low kinetic energy.<sup>10,11</sup>

#### IV. TRIPLE-POMERON EFFECTS

A number of authors have argued recently that the rise in the p-p total cross section can be understood as the result of the appearance of large-mass diffraction dissociation.<sup>12-15</sup> This is based on the observation that the contribution of such processes to  $\sigma_{tot}$  is given by integrating the inclusive cross section corresponding to Fig. 8 over the region of phase space where both  $s$  and  $s/M^2$  are large. Treating the pomeron trajectory as approximately flat and equal to 1, one finds a contribution proportional to  $\langle g_p \rangle \log s$ , where  $\langle g_p \rangle$  is a certain average value of the triple-pomeron vertex. The measured value of  $\langle g_p \rangle$  is about of the order of magnitude of the observed slope of  $\sigma_{tot}$ .

We would like to criticize this explanation on several different grounds. First, there are two numerical problems: (1) The predicted threshold for the increase seems to occur at too low an energy. Triple-pomeron behavior is, strictly speaking, the high-energy tail of the pomeron-particle total cross section, and the latter has the form shown in Fig. 9 [taken from Ref. (16)]. This gives  $M_0^2 \approx 4 \text{ GeV}^2$  as the threshold in fireball mass squared, and even taking  $\Delta_p \approx 2-3$  units as the minimum rapidity gap between the proton and the fireball we would have a p-p total cross section which begins to rise at

$$Y = \Delta_p + \log M_0^2 \approx 3-4 .$$

Experimentally, the rise does not begin until  $Y \approx 6$ . (2) The measured magnitude of  $\langle g_p \rangle$  corresponding to Fig. 9 is too low by



about a factor 2 to account for the behavior of  $\sigma_{tot}$ .

A further difficulty is that Fig. 9 is really a smooth curve and contains no definite threshold. If  $\sigma_p$  is parametrized as a flat background with a low-M resonant effect superimposed, the "triple-pomeron threshold" is just  $\Delta_p$ , which is much too low. It might be argued that this early rise is masked by other (decreasing) terms in  $\sigma_{tot}$ , but one must then consider a more complete model of the cross section.

If one does in fact look at  $\sigma_{tot}$  in more detail, a further objection arises within nonabsorbed perturbative models of the pomeron,<sup>13,17</sup> as described in Prof. Frazer's talk. In his notation, the total cross section is represented by the sum shown in Fig. 10. It is necessary to distinguish a bare pomeron ( $P_0$ ) which is generated by events with no large rapidity gaps in the unitarity sum. The relation between the two different kinds of pomeron is that the physical pomeron intercept  $\alpha_p(0)$  is the zero of a denominator function,

$$D(J) = J - \alpha_0 - e^{-(J-\alpha_0)\log M_0^2} \times \int \frac{dt}{16\pi} \frac{G^2(t) e^{-\Delta_p(J-2\alpha_p(t)+1)}}{J - 2\alpha_p(t) + 1}, \quad (7)$$

where  $\alpha_0$  is the bare intercept and  $G$  is the P-P- $P_0$  triple-Regge coupling. The origin of this formula is formally the same as in the antibaryon model above; cf. the denominator of Eq. (6). The last term is a two-pomeron loop integral, with appropriate threshold factors.

The absence of a threshold within the pomeron-particle absorptive part, as described above, corresponds to setting  $M_0 = 1$  in Eq. (7). In this case the remaining exponential factor,

$e^{-\Delta_p J}$ , is not sufficient to produce physically significant complex poles. The importance of this circumstance is that the only other Regge singularities of the model are the leading pole and a two-pomeron branch cut with a positive discontinuity, so if there are no complex poles the cross section must fall. This statement seems paradoxical, since one might think an arbitrarily large rise can be arranged by making  $G$  large enough. However, the form of  $D(J)$  in (7) implies that the "renormalization" of pomeron pole intercept,  $\alpha_p(0) - \alpha_0$ , increases with  $G$ . Since  $\alpha_p(0) \leq 1$ , an increase in  $G$  necessarily lowers  $\alpha_0$ , and makes the short-range correlation

component of  $\sigma_{\text{tot}}$  fall faster. Careful examination of the competing tendencies confirms the theorem that the only possible way to get (even a temporary) increase in  $\sigma_{\text{tot}}$  is via complex poles.

#### FOOTNOTES AND REFERENCES

1. D. Sivers and F. von Hippel, Argonne preprint ANL/HEP 7323 (1973).
2. M. Suzuki, University of California, Berkeley preprint (1973).
3. T. K. Gaisser and C.-I. Tan, Brookhaven preprint BNL 18070 (1973).
4. G. F. Chew, T. Rogers, and D. R. Snider, Phys. Rev. D2, 765 (1970).
5. G. F. Chew and D. R. Snider, Phys. Letters 31B, 75 (1970).
6. M. Antinucci et al., Nuovo Cimento Letters 8, 121 (1973). Note that the  $\bar{p}$  cross sections discussed in this paper include the decay products of antihyperons.
7. Figure 2, which is taken from Ref. 6, is really the integrated  $\bar{B}$  inclusive cross section, and is equal to  $\sigma_{\bar{B}}$  provided we make the reasonable assumption that not more than one anti-baryon is produced per event.
8. G. F. Chew and J. Koplik, in preparation.
9. U. Amaldi et al., Phys. Letters 44B, 112 (1973); S. R. Amendolia et al., *ibid.* 44B, 119 (1973).
10. J. S. Ball and G. F. Chew, Phys. Rev. 109, 1385 (1957).
11. R. J. N. Phillips, Rev. Mod. Phys. 39, 681 (1967).
12. A. Capella, M.-S. Chen, M. Kugler, and R. D. Peccei, Phys. Rev. Letters 31, 497 (1973); A. Capella and M.-S. Chen, SLAC-PUB-1252 (1973).
13. W. R. Frazer, D. R. Snider, and C.-I. Tan, La Jolla preprint UCSD-10P10-127 (1973).
14. D. Amati, L. Caneschi, and M. Ciafaloni, CERN TH.1676 (1973).
15. G. F. Chew, Phys. Letters 44B, 169 (1973); M. Bishari and J. Koplik, *ibid.* 44B, 175 (1973).
16. A. B. Kaidalov, V. A. Khoze, Yu. F. Pirogov, and N. L. Ter-Isaakyan, Phys. Letters 45B, 493 (1973).
17. M. Bishari, G. F. Chew, and J. Koplik, Lawrence Berkeley Laboratory reports LBL-2129 and LBL-2130 (1973).

#### FIGURE CAPTIONS

- Fig. 1. The pion-exchange multiperipheral model.
- Fig. 2. The antibaryon cross section as a function of energy.
- Fig. 3. Diagram controlling the  $\bar{B}\bar{B}$  threshold.
- Fig. 4. Production of two  $\bar{B}\bar{B}$  pairs.
- Fig. 5. The  $N\text{-}\bar{B}\bar{B}$  pair cross section as a function of energy.
- Fig. 6. Regge poles of the  $\bar{B}\bar{B}$  model.
- Fig. 7. Total cross section and ratio of real to imaginary part in the  $\bar{B}\bar{B}$  model.

- Fig. 8. Large-mass diffraction dissociation.
- Fig. 9. The pomeron-proton total cross section.
- Fig. 10. Perturbative model of the pomeron.

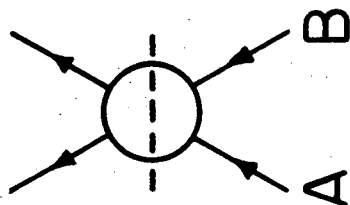
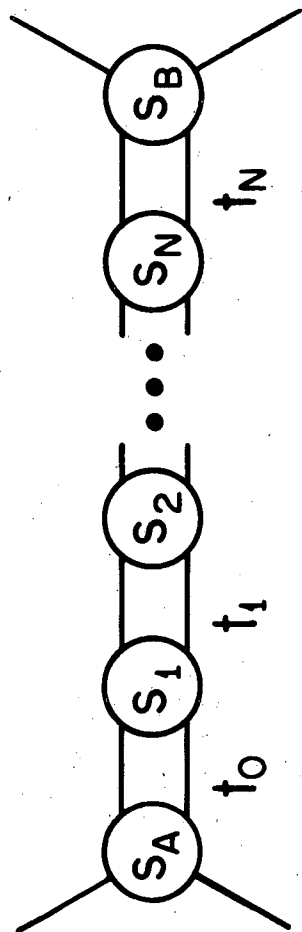


Fig. 1

XBL739 - 4124

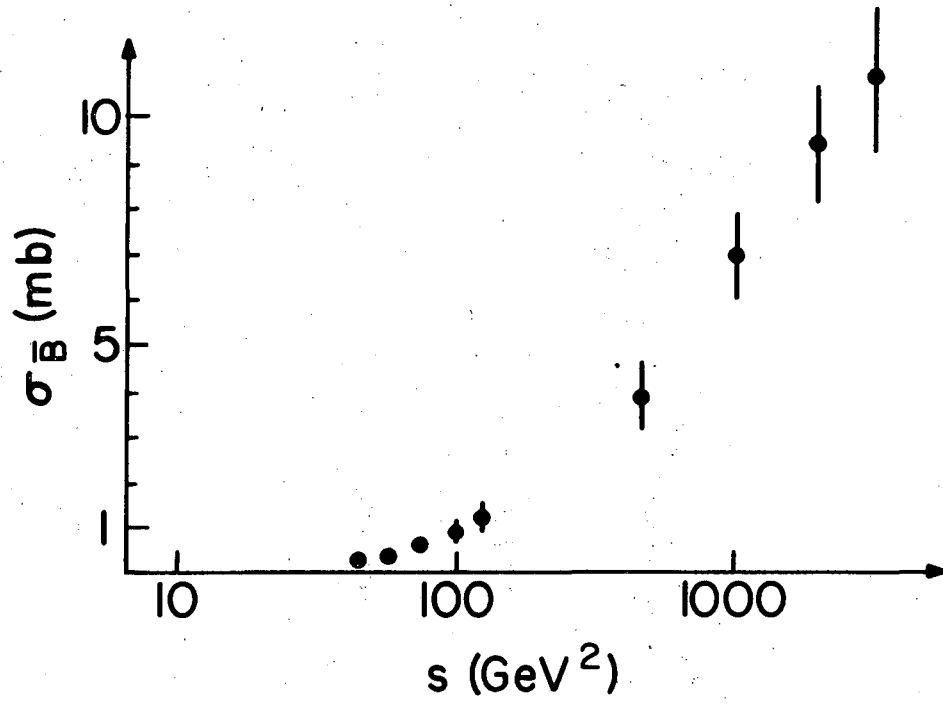


Fig.2

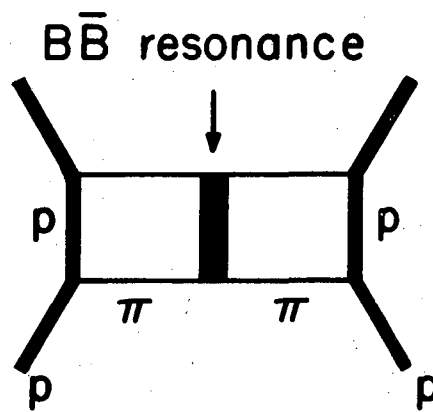


Fig.3

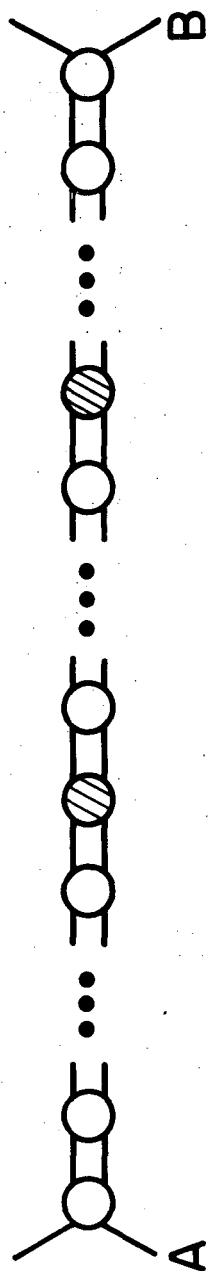


Fig. 4a

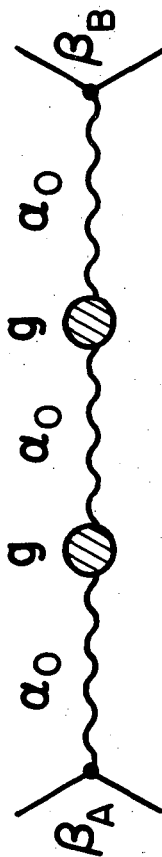


Fig. 4b

XBL739-4126

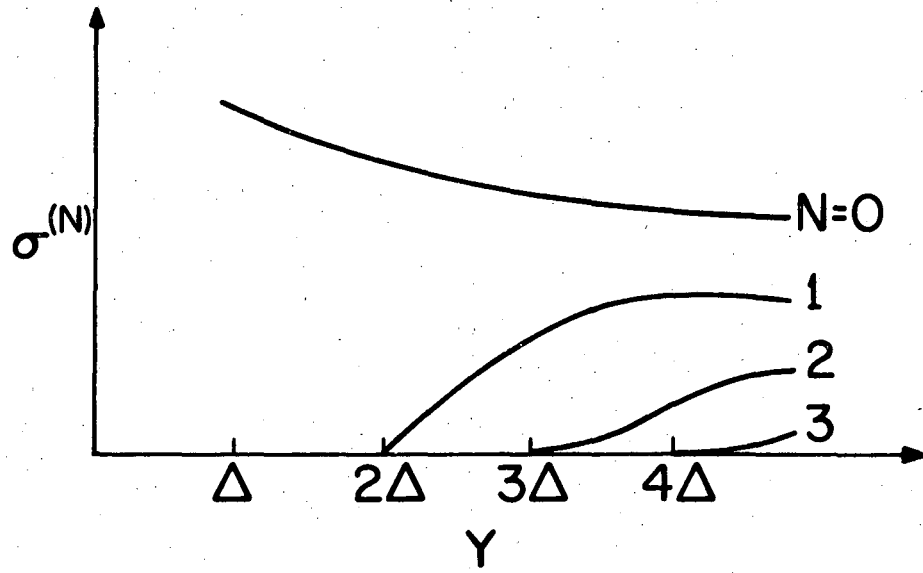


Fig.5

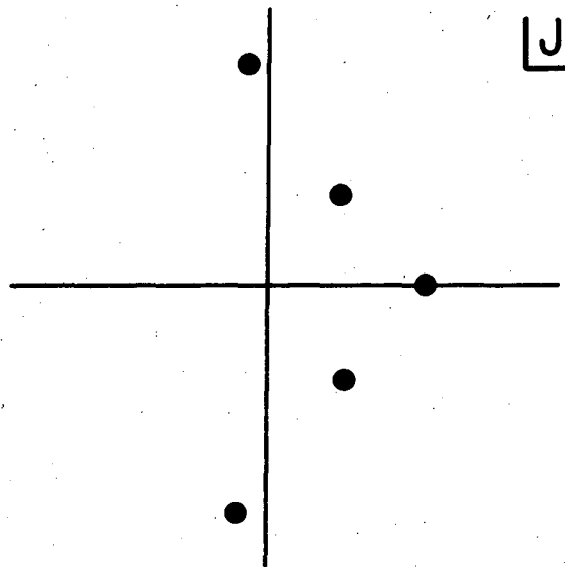


Fig.6

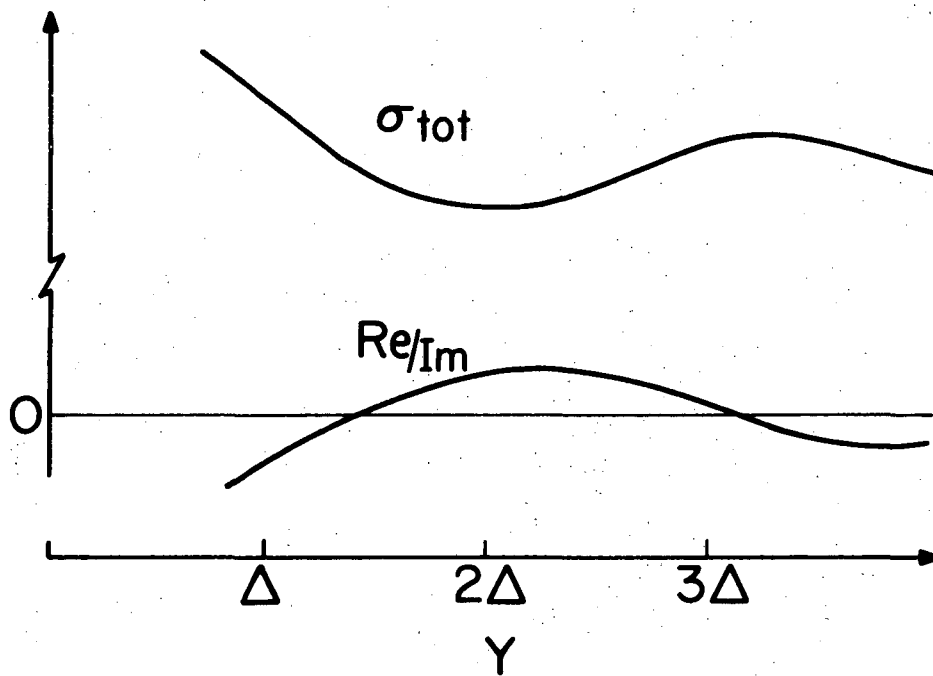


Fig. 7

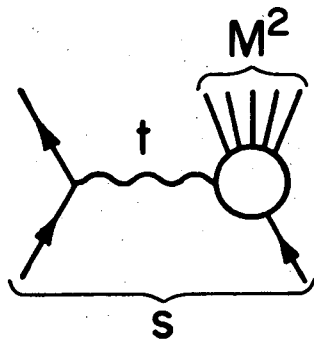


Fig. 8



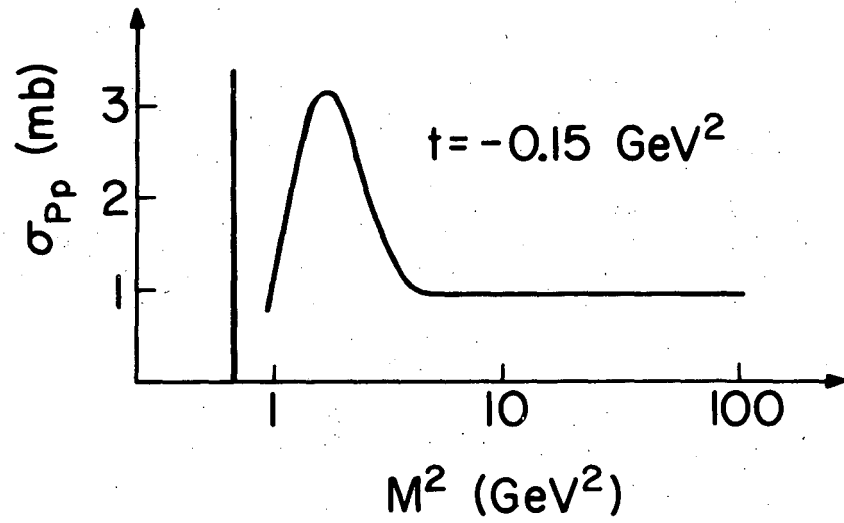


Fig. 9

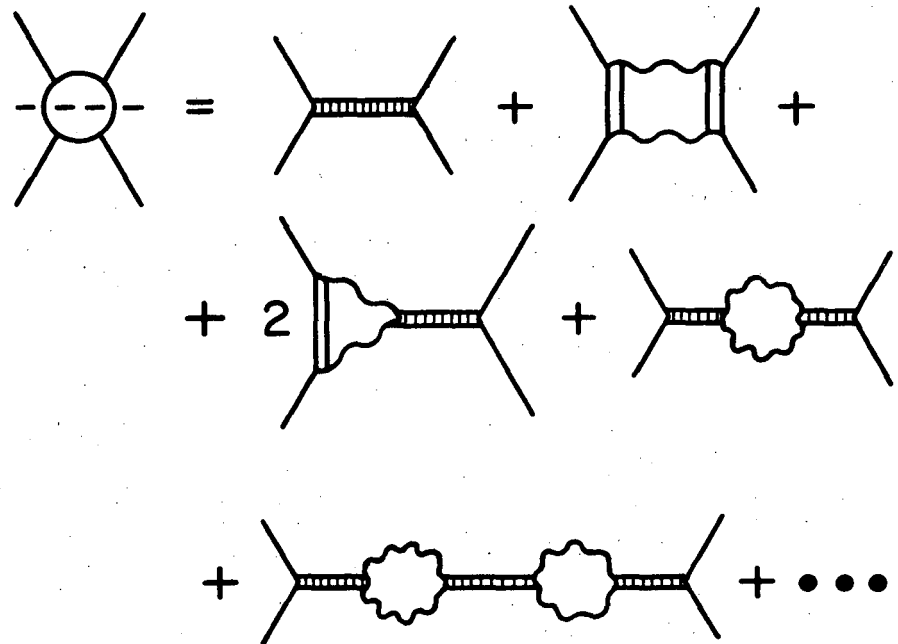


Fig. 10

XBL739-4129

LEGAL NOTICE

*This report was prepared as an account of work sponsored by the United States Government. Neither the United States nor the United States Atomic Energy Commission, nor any of their employees, nor any of their contractors, subcontractors, or their employees, makes any warranty, express or implied, or assumes any legal liability or responsibility for the accuracy, completeness or usefulness of any information, apparatus, product or process disclosed, or represents that its use would not infringe privately owned rights.*

TECHNICAL INFORMATION DIVISION  
LAWRENCE BERKELEY LABORATORY  
UNIVERSITY OF CALIFORNIA  
BERKELEY, CALIFORNIA 94720